Corrosion Science 98 (2015) 592–604

Contents lists available at ScienceDirect

Corrosion Science

journal homepage: www.elsevier.com/locate/corsci

Modelling of the kinetics of pitting corrosion by metal dusting

Aurélien Fabas[a], Daniel Monceau[a,*], Sébastien Doublet[b], Aurélie Rouaix-Vande Put[a]

[a] Université de Toulouse, Institut Carnot CIRIMAT, INPT-ENSIACET, 4 allée Emile Monso, BP-44362, 31432 Toulouse Cedex 4, France
[b] Air Liquide R&D, Paris-Saclay Research Center, 1 chemin de la porte des loges, BP-126, 78354 Jouy-en-Josas Cedex, France

ARTICLE INFO

Article history:
Received 14 February 2015
Accepted 29 May 2015
Available online 6 June 2015

Keywords:
A. Stainless Steel
B. Modelling studies
C. High temperature corrosion
C. Pitting corrosion

ABSTRACT

Commercial 800HT alloy was exposed to 49.1%H_2–12.8%CO–3.1%CO_2–1.6CH_4–33.4%H_2O gas at 21 bars and 570 °C up to 5000 h. Metal dusting attack by pitting was observed. The kinetics parameters were identified to be the incubation time, pit density and individual pit growth rate. These parameters were introduced in a nucleation-growth model to simulate the pitted surface area kinetics. This model was then extended to the volume considering several geometrical hypotheses. Considering only surface coalescence of the pits without their volume coalescence allowed to correctly reproduce the experimental mass loss kinetics. An even simpler conservative model was proposed for an easy lifetime modelling.

1. Introduction

When Ni-, Fe- or Co-based alloys are exposed to highly carburising atmospheres ($a_c > 1$), a catastrophic corrosion may take place [1,2]. This phenomenon, called "metal dusting", happens at a temperature in the range of 400–800 °C. It is characterised by the disintegration of the alloy into a dust of fine metallic particles and graphitic carbon, named "coke". Mechanisms have been proposed to explain metal dusting attack of Fe-based [1,3,4,6] and of Ni-based alloys [5,7]. Metal dusting is a very complex type of corrosion which depends on the nature of the alloy [8,9], its microstructure [10,11] and composition [12,13]. Of course, it is also greatly influenced by the atmosphere composition [3,8,14], the temperature [15,16] and the overall pressure [17,18]. Due to the low oxygen partial pressure (below 10^{-20} bar), only very stable oxides such as chromia, alumina, silica or some spinels can form. Chromia and alumina are well known for limiting or preventing carbon ingress into the alloy. In this case, the fast degradation due to metal dusting occurs after an incubation time, which duration depends on the quality and stability of the protective oxide scale. An alloy which can form such an oxide scale will be corroded when the scale fails to protect the material, due to cracks, spalls or other defects. The alloy will be degraded locally, via a pitting-type mechanism [4,8,9,19]. Even if pitting is always noticed, only few studies focus on this phenomenon [19–23]. Moreover, as far as the authors know, the kinetics of metal dusting by pitting has never been modelled, despite existing modelling efforts in other type of pitting corrosion in aqueous environments [24]. The present work aims to propose a simple kinetic model for pitting-type metal dusting corrosion, which could be used to quantify the degradation. It is based on simple optical surface observations on 800HT commercial alloy. The mass change is also assessed using a study of pit morphology characterised on cross sections. The limits of the model and the physical phenomenon from which pitting kinetics is evaluated are discussed.

2. Materials and experiments

The chemical composition of the 800HT alloy studied in the present work was obtained by EDS. Its composition is presented in Table 1. The 800HT samples were cut in a commercial rod to obtain disc specimens with a diameter and a thickness of approximately 14 mm and 1.6 mm respectively. A hole was drilled at the centre of each specimen. These samples were held by alumina sticks in the subsequent exposure test. One side of the sample faces the sample holder – called "internal side" below: the other side faces the inner surface of the furnace – called "external side" below. The specimens were chamfered to limit edge effects. Samples were mechanically ground to a P600 grit finish, and ultrasonically cleaned in acetone and in ethanol, and dried before the experiment.

The isothermal corrosion test was performed in a vertical furnace. Three 800HT samples were exposed simultaneously to a 49.1%H_2–12.8%CO–3.1%CO_2–1.6%CH_4–33.4%H_2O gas mixture at 570 °C and 21 bars. This gas mixture was obtained by first creating a mixture of H_2, CO, CO_2 and CH_4 using pure pressurised gases and

* Corresponding author at: CIRIMAT UMR5085 CNRS-INPT-UPS, ENSIACET, 4, allée Emile Monso, BP-44362, 31030 Toulouse Cedex 4, France. Tel.: +33 5 34 32 34 22; fax: +33 5 34 32 34 22.
E-mail address: daniel.monceau@ensiacet.fr (D. Monceau).

http://dx.doi.org/10.1016/j.corsci.2015.05.061
0010-938X/

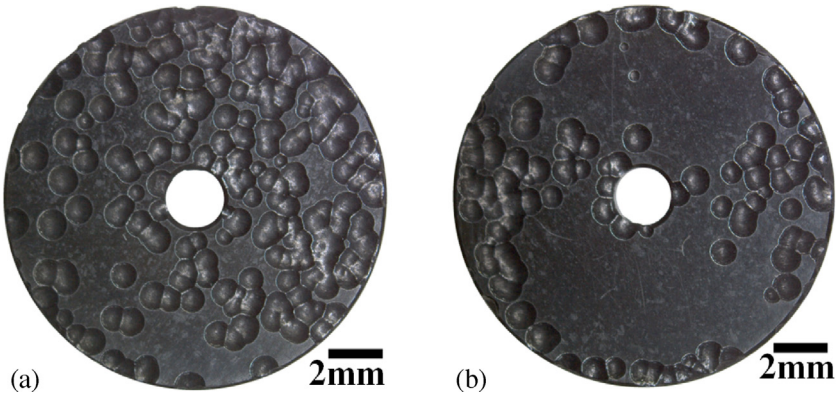

Fig. 1. Pictures of (a) external and (b) internal side of 800HT sample #3 after 4941 h in H_2–CO–CO_2–CH_4–H_2O at 570 °C, 21 bar.

mass flow controllers on each line for the setting of the dry gas composition. Then, the water was introduced in the preheated gas via a calibrated High Pressure Liquid Chromatography (HPLC) pump. The homogenisation of the gas composition and temperature was promoted by flowing the atmosphere through a ceramic foam at the furnace inlet. The total system pressure was controlled downstream of the furnace via a backpressure regulator placed on the outlet dry gas line. The amount of water was controlled by weighting the condensed water at the equipment outlet. The linear gas flow rate was adjusted to 0.28 cm/s and 2290 scc/h/sample. In the aforementioned atmosphere, the carbon activity a_c, calculated from the synthesis gas reaction, and the partial pressure of oxygen P_{O2}, calculated from the water decomposition reaction, were 32.0 and 7.1×10^{-26} bar respectively, using thermodynamical data from Ref. [25].

The three 800HT samples were removed approximately every 500 h. After being cleaned ultrasonically in ethanol and being dried, they were weighted on a Sartorius CPA225DOCE balance with a precision of 0.01 mg. Pictures (with a precision of 7 μm/pixel) of each sample were also taken on both faces thanks to a Zeiss Stemi 2000-C Stereomicroscope, and further analysed with ImageJ software. The entire surface was analysed except a 1 mm thick hoop, which was systematically removed from the sample edges. This was done in order to limit any edge effect in the surface analysis. It was done for the external edge of the sample as well as for the internal edge, i.e. around the central hole. Pit diameter was averaged by measurements on numerous pits. The averaged, maximum and minimum incubation times were determined by extrapolating backwards (to zero size) the experimental kinetics of pit diameter growth.

After the exposure test, each sample was characterised by X-ray diffraction (XRD) on a Seifert 3000TT apparatus with a copper anti-cathode (λ = 1.54056 Å). XRD were carried out using a small incidence angle of 2°. Optical microscopy, Raman spectroscopy and scanning electron microscopy (SEM) were performed on one side and on cross section for each sample. The optical microscope used in this study was a Nikon Eclipse MA200. Raman spectroscopy was done using a Labram HR 800 Yvon Jobin spectrometer equipped with a confocal microscope (magnifications are 10×, 50× and 100×) using a 514 nm argon ion laser. SEM observations were carried out using a LEO 435 VP using secondary (SE) and backscattered electrons (BSE) modes. EDS analyses were done using an IMIX system from PGT. Cr-carbides were revealed by etching in Murakami reagent (1 g $K_3Fe(CN)_6$, 1 g KOH, 10 mL H_2O) at room temperature during 30 s.

Table 1
Chemical composition of the 800HT alloy used in this study, measured by EDS.

Element	Fe	Ni	Cr	Ti	Al	Si	Mn	Cu
%at	Bal.	28.0	22.0	0.8	1.5	1.2	0.8	0.2

3. Results

3.1. Overview

The global behaviour was found to be the same for all samples. Pitting was first detected after 1147 h of exposure (second removal) on both sides. The external face was the most severely attacked for all specimens. The pits had a circular shape and were not randomly distributed as it can be seen in Fig. 1. Relevant weight mass loss occurred also after 1147 h (Fig. 2). The oxide scale was mainly constituted of Cr_2O_3. $(Fe,Cr)_3O_4$ spinel oxide, $(Cr,Fe)_{23}C_6$ carbides and amorphous and crystallised carbon were also detected by XRD and Raman spectroscopy (Fig. 3). Among the numerous areas analysed by Raman spectroscopy, no change on the composition of chromia, spinel oxide or of the proportion of each oxide was noticed. Only carbon proportion was observed to vary.

3.2. Mass change

No significant mass change occurred before 1147 h of exposure (Fig. 2). Sample #1, definitively removed after 1987 h of exposure, was characterised by a shorter incubation time than samples #2 and #3, definitely removed after 3472 h and 4941 h, respectively. Samples #2 and #3 presented the same incubation time and an almost linear mass loss kinetics after 2322 h and 3472 h, respectively. This

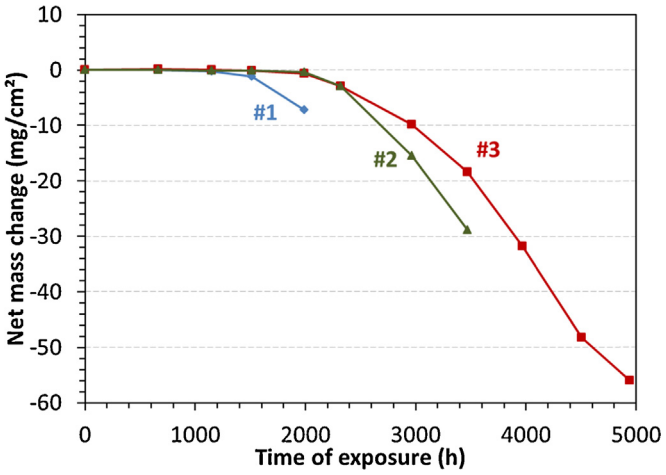

Fig. 2. Net mass change of the 800HT samples in H_2–CO–CO_2–CH_4–H_2O at 570 °C, 21 bar.